

# Deep Instruction Tuning for Segment Anything Model

Xiaorui Huang<sup>1,2</sup> Gen Luo<sup>1</sup> Chaoyang Zhu<sup>3</sup> Bo Tong<sup>1</sup> Yiyi Zhou<sup>1,2</sup> Xiaoshuai Sun<sup>1,2</sup> Rongrong Ji<sup>1,2</sup>

## Abstract

*Segment Anything Model* (SAM) exhibits powerful yet versatile capabilities on (un) conditional image segmentation tasks recently. Although SAM can support various segmentation prompts, we note that, compared to point- and box-guided segmentation, it performs much worse on text-instructed tasks. We argue that deep text instruction tuning is key to mitigate such shortcoming caused by the shallow fusion scheme in its default light-weight mask decoder. In this paper, two *deep instruction tuning* (DIT) methods are proposed, one is end-to-end and the other is layer-wise. With these tuning methods, we can regard the image encoder of SAM as a stand-alone vision-language learner in contrast to building another deep fusion branch. Extensive experiments on three highly competitive benchmark datasets of referring image segmentation show that a simple end-to-end DIT improves SAM by a large margin, with layer-wise DIT further boosts the performance to state-of-the-art. Our code is anonymously released at: <https://github.com/wysnzzz/DIT>.

## 1. Introduction

Motivated by the great success of large language models (Ouyang et al., 2022; Touvron et al., 2023), Kirillov et al. (2023) recently propose a *Segment Anything* project to build a foundation model for image segmentation, termed *Segment Anything Model* (SAM). SAM demonstrates an impressive yet versatile capacity on various image segmentation tasks (Long et al., 2015; He et al., 2017; Kirillov et al., 2019) by pre-training on over one billion masks. Moreover,

<sup>1</sup>Key Laboratory of Multimedia Trusted Perception and Efficient Computing, Ministry of Education of China, Xiamen University, 361005, P.R. China. <sup>2</sup>Institute of Artificial Intelligence, Xiamen University, 361005, P.R. China. <sup>3</sup>The Department of Computer Science and Engineering, The Hong Kong University of Science and Technology, Kowloon, Hong Kong. Correspondence to: Yiyi Zhou <[zhouyiyi@xmu.edu.cn](mailto:zhouyiyi@xmu.edu.cn)>.

<sup>1</sup>Three methods are trained using the frozen ViT-B encoder.

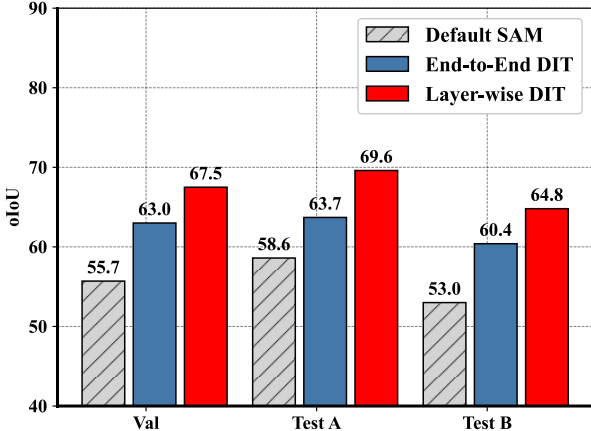


Figure 1: The comparison among the default fusion scheme of SAM (with ViT-B) and our deep instruction tuning methods on RefCOCO (Yu et al., 2016), i.e., the end-to-end and layer-wise ones, respectively<sup>1</sup>. In SAM, the text prompts only interact with the visual tokens with the shallow mask decoder, which is insufficient for cross-modal fusion and text-guided segmentation. Our simple deep tuning methods can improve the performance by a large margin without significantly changing the architecture of SAM.

it can support interactive segmentation conditioned on various input prompts, such as *points*, *boxes* or *texts*.

However, for SAM to follow text instructions, as shown in Fig. 1, it only achieves 55.7 accuracy when fine-tuned on RefCOCO (Yu et al., 2016), which is much inferior than following points or boxes (Kirillov et al., 2023). Text instructions naturally exhibit linguistic ambiguities, while location prompts (points and boxes) are precise. Even worse, the shallow fusion scheme in SAM further aggravates such weakness and degrades its multi-modal ability.

More concretely, for either point, box or text, input prompt is first encoded by the prompt encoder of SAM, then it is directly fed into the light-weight encoder of SAM for mask prediction. In SAM, prompts can only interact to a limited extent with visual tokens via two cross-attention layers in its mask decoder (Kirillov et al., 2023). Although such mechanism is well suited for point and box prompts which are relatively easy to follow, it is insufficient for SAM to infer the intentions behind texts step-by-step. Oftentimes,

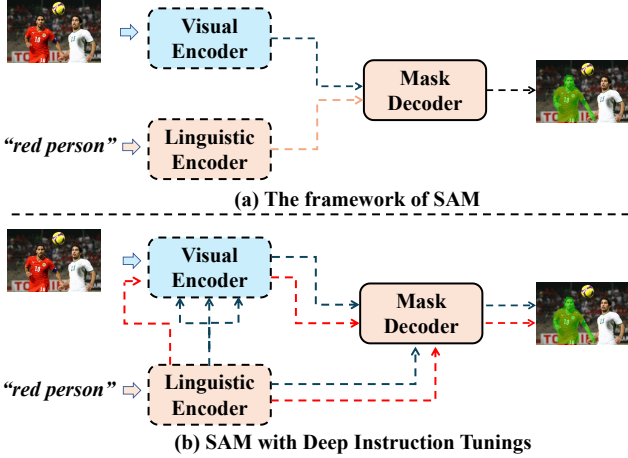


Figure 2: Illustrations of the default fusion of SAM (a) and our *deep instruction tuning* (DIT) methods (b), *i.e.*, the end-to-end (red) and layer-wise (blue) ones. Compared with the default shallow fusion, DITs regard the visual encoder as a deep multi-modal learner for cross-modal fusion and visual feature learning, thereby achieving the full interactions between text and image for text-guided SAM.

SAM needs to resolve linguistic ambiguity first through the attributes and relationships of the referent, then the object can be masked using its powerful and class-agnostic segmentation ability. To this end, we argue that

*“Deep text instruction tuning is essential for SAM.”*

To validate this argument, we propose two *deep instruction tuning* (DIT) methods for SAM. Different from existing RIS models (Huang et al., 2020; Deng et al., 2021; Kim et al., 2022; Li et al., 2022) that build deep fusion branches upon image encoders, we focus on improving text instruction following ability of SAM without modifying its structure. In particular, we draw inspiration from *prompt tuning* (Zhou et al., 2022a;b) and directly extend SAM to a deep vision-language model. Enabled by the flexibility of Transformer-based encoder (Dosovitskiy et al., 2020), we convert prompt words to input tokens and concatenate them with visual tokens for deep multi-modal fusion and feature learning, which forms the first DIT scheme in this paper, we termed *end-to-end* one (E-DIT). As shown in Fig. 1 and Fig. 2, this simple method improves SAM by a large margin, *i.e.*, +11.8% on RefCOCO *val*. To further enhance instruction learning, we also propose a layer-wise instruction tuning method (L-DIT) that independently projects and inserts the text words into each layer of SAM. This layer-wise method has a similar principle with *soft prompt tuning* (Jia et al., 2022). The difference is that the inserted tokens are the projected text embeddings that vary across examples, instead of task-specific and parameterized prompt tokens.

With the proposed DIT methods, we apply SAM to the pop-

ular text-guided *Referring Image Segmentation* (RIS) (Liu et al., 2023d;b), and term the new models as DIT-SAMs. Extensive experiments are conducted on three highly competitive benchmarks, namely RefCOCO (Yu et al., 2016), RefCOCO+ (Yu et al., 2016) and RefCOCOg (Mao et al., 2016; Nagaraja et al., 2016). The experimental results not only show the great advantages of DIT-SAMs over SAM, *e.g.*, up to 11.6% improvement on RefCOCO *testA*, but also confirm the competitiveness of DIT-SAM as a stand alone RIS model. Overall, we provide a fast and feasible solution to extend SAM’s modal-modal ability.

To summarize, our contributions are three-fold:

- We reveal the key drawbacks of SAM in terms of text-guided segmentation and argue that deep text instruction tuning is key to success.
- We propose two simple yet effective *deep instruction tuning* (DIT) methods for SAM, which are end-to-end and layer-wise, respectively. These DIT methods provide feasible solutions to efficiently extend the multi-modal capabilities of SAM.
- The proposed DIT-SAMs not only greatly outperforms SAM on RIS benchmarks, but also shows great competitiveness against existing SOTA methods of RIS.

## 2. Related Work

### 2.1. Image Segmentation

As a fundamental task in computer vision, image segmentation (Ronneberger et al., 2015; Long et al., 2015; He et al., 2017; Badrinarayanan et al., 2017) requires pixel-level understanding of a given image. Various segmentation-related tasks have been investigated, such as *semantic segmentation* (Long et al., 2015; Badrinarayanan et al., 2017; Chen et al., 2017; He et al., 2017; Xie et al., 2021), which categorizes individual pixels into a predetermined set of classes, and *instance segmentation*, primarily concerns itself with the recognition and delineation of distinct object instances (He et al., 2017; Tian et al., 2020; Wang et al., 2020), *Panoptic segmentation*, which merges semantic and instance segmentation tasks by assigning class labels and individual instance identification (Kirillov et al., 2019; Li et al., 2019). Recently, the Segment Anything project (Kirillov et al., 2023) proposes a powerful model for image segmentation, termed SAM. This project includes the creation of an unprecedentedly large segmentation dataset so SAM is trained with about 1 billion image-mask pairs. Due to this large-scale pre-training, SAM exhibits robust and versatile performance across various segmentation challenges. Notably, SAM is also capable of handling different types of prompts for conditional segmentation, such as point, box and text. However,

as mentioned above, SAM works much worse with texts than the other types of prompts.

## 2.2. Referring Image Segmentation

*Referring image segmentation* (RIS) is a text-conditioned segmentation task that grounds the referent with binary masks according to the given natural language expression (Hu et al., 2016). Early research in RIS (Yu et al., 2016; Liu et al., 2019) typically adopts a two-stage pipeline and frames RIS as a problem of region-text matching. One-stage RIS models (Liu et al., 2017; Li et al., 2018; Margffoy-Tuay et al., 2018) recently garner growing attention from both academia and industry. In these one-stage models, text features are often embedded into the vision network and directly output the mask of the referent. Inspired by the success of the Transformer, various Transformer-based RIS models (Zhu et al., 2022; Hu et al., 2023; Liu et al., 2023c;a; Wu et al., 2023a; Xu et al., 2023a) are recently proposed to improve the multi-modal reasoning ability for RIS. VLT (Ding et al., 2022) and SeqTR (Zhu et al., 2022) use an encoder-decoder framework to fuse visual and language inputs into the decoder. ReSRT (Kim et al., 2022) employs two separate Transformer encoders to handle two different modalities. LAVT (Yang et al., 2022) add a ladder-side language pathway for the cross-modal fusion of text features and visual tokens. UniLSeg (Liu et al., 2023f) employs symmetric and multi-modal Transformer networks for multi-modal fusion, while UNINEXT (Yan et al., 2023) utilizes a multi-modal Transformer encoder for the same purpose. LISA (Lai et al., 2023) and SEEM (Zou et al., 2024) focus on text-instructed open-world segmentation, they introduce much more training data and the use of giant LLMs (e.g., LLaMA-7B (Touvron et al., 2023)). Apart from network design, recent research (Luo et al., 2020b; Li & Sigal, 2021; Liu et al., 2023f) also emphasizes early fusion to enhance performance.

## 2.3. Prompt Tuning

With the ever increasing parameter size of pre-trained models (Devlin et al., 2018; Dosovitskiy et al., 2020; Touvron et al., 2023), the direct fine-tune on downstream tasks becomes prohibitively expensive. In this case, *prompt tuning* (Gu et al., 2021; Liu et al., 2021; Wei et al., 2021; Han et al., 2022) is proposed to use hand-craft or learnable prompt tokens to mitigate distribution shifts between pre-training and downstream tasks. The significant achievements of prompt tuning in natural language processing (NLP) have also inspired its application in the fields of computer vision and vision-language research (Liu et al., 2023e). CoOp (Zhou et al., 2022b) remains CLIP parameters untouched and uses learnable parameters as soft prompts for the input text, thereby maximizing CLIP’s zero-shot retrieval capabilities. To address overfitting issue on base classes, CoCoOp

(Zhou et al., 2022a) proposes instance adaptation by incorporating the visual features of each image into the learnable prompts. RPO (Lee et al., 2023) enhances the robustness of VL models by using masked attention to prevent the added learnable embeddings from altering the original internal representations of the model. More recently, Wu et al. (Wu et al., 2023b) propose a method of *approximated prompt tuning* to reduce the additional cost of adding prompt tokens.

## 3. Method

### 3.1. Problem definition

*Referring image segmentation* aims to segment the referred object in an image  $I$  conditioned on the paired language expression  $T$ , its objective is formulated as

$$\arg \min_{\theta} \mathcal{L}(\mathcal{F}(I, T; \theta), M), \quad (1)$$

where  $\mathcal{F}$  denotes the model with its parameters  $\theta$ ,  $M \in \mathbb{R}^{H \times W}$  is the ground-truth mask, and  $\mathcal{L}$  is the canonical cross entropy loss.

To achieve this task, SAM (Kirillov et al., 2023) first extracts vision and text features through its vision and language encoder, based on which the light-weight decoder takes as input to predict the binary masks. Thus, the model  $\mathcal{F}$  instantiated by SAM is

$$\mathcal{F}(I, T; \theta) = \mathcal{F}_d(\mathcal{F}_v(I), \mathcal{F}_t(T)), \quad (2)$$

where  $\mathcal{F}_v$ ,  $\mathcal{F}_t$  and  $\mathcal{F}_d$  refer to visual backbone, language encoder and mask decoder, respectively.

The mask decoder is very lightweight and only contains two cross-attention layers, which are in charge of both mask decoding and multi-modal interactions. In this case, SAM can be regarded as one of the late-fusion models which proved to be less effective than the early-fusion ones (Luo et al., 2020a;b; Zhu et al., 2022; Liu et al., 2023d) in addressing the complicated multi-modal reasoning tasks. Meanwhile, due to a lack of training on cross-modal data, text-guided SAM performs worse than the point- or box-guided SAM, leading to much inferior cross-modal abilities than existing SOTA methods in RIS (Zhu et al., 2022; Liu et al., 2023d).

We introduce Deep Instruction Tuning (DIT) for SAM to better follow the intentions reflected in the language expression  $T$ . In particular, DIT keeps the whole SAM architecture unchanged and directly uses the image encoder as a strong multi-modal fusion network. The text prompts can continually interact with the visual contents through the whole feature learning process, helping SAM progressively locate the referent. Specifically, SAM with DIT can be then formulated as

$$\mathcal{F}(T, I; \theta) = \mathcal{F}_d(\mathcal{F}_v(I, \phi(\mathcal{F}_t(T))), \mathcal{F}_t(T)). \quad (3)$$

Here,  $\phi(\cdot)$  is a mapping function to project the text features onto visual space.

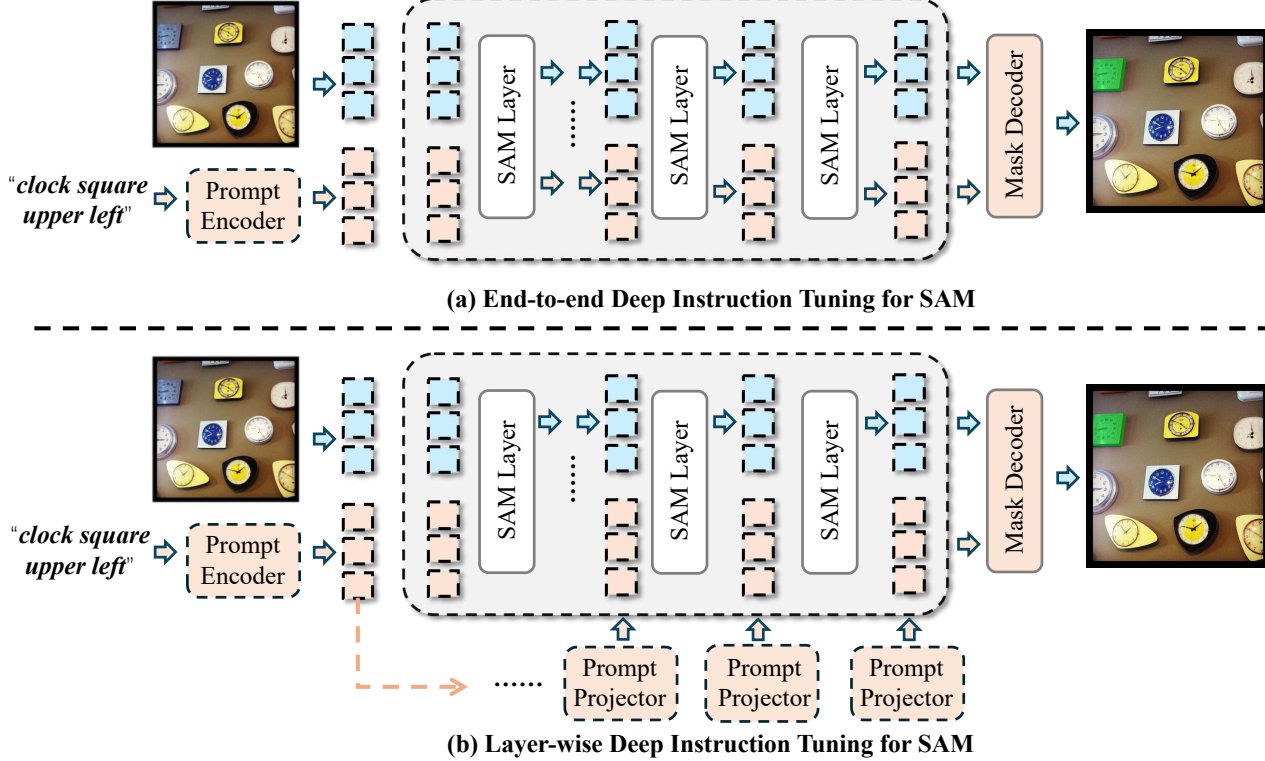


Figure 3: Overall pipeline of Deep Instruction Tuning (DIT). We propose (a) End-to-end DIT (E-DIT) that appends language instructions before visual features to achieve early-fusion for enhancing multi-modal reasoning capability; (b) Layer-wise DIT (L-DIT) that layer-wisely projects to interact with the existing sequences in the well learned semantic space.

### 3.2. End-to-end Instruction Tuning

One straightforward solution for SAM is to directly feed the prompt words to its ViT-based image encoder. Due to the flexibility of Transformer architecture, the text features can be also regarded as additional input tokens for feature transformations. This attempt is also validated in previous VL works like ViLT (Kim et al., 2021), and has a similar principle with the popular prompt tuning (Jia et al., 2022).

Here, we term this DIT solution as the end-to-end tuning, abbreviated as E-DIT. Concretely, given a text description  $T$ , we first use the language encoder, *i.e.*, BERT (Devlin et al., 2018), to extract their representations, denoted as  $\mathbf{F}_t \in \mathbb{R}^{l \times d}$ , where  $l$  denotes the length of description. The visual features after the patch embedding layer is denoted as  $\mathbf{F}_v^0 \in \mathbb{R}^{m \times d}$ . Here,  $m = HW/P^2$  is the number of patches, where  $H \times W$  is the image resolution and  $P^2$  is the patch size. Afterwards, we use a linear layer to project  $\mathbf{F}_t$  onto the visual semantic space of SAM, and obtain  $\mathbf{F}_t^0$ :

$$\mathbf{F}_t^0 = \mathbf{F}_t \mathbf{W}_0 + b_0, \quad (4)$$

where  $\mathbf{W}_0 \in \mathbb{R}^{d \times d}$  and  $b_0 \in \mathbb{R}^d$  denote the projection weight and the bias term, respectively.

These text tokens and image patches are then processed by the following Transformer layers of the encoder for both

image feature learning and cross-modal fusions. The output image features  $\mathbf{F}_v^n$  alone with the text features  $\mathbf{F}_t$  are fed to the lightweight mask decoder. In this case, E-DIT is formulated by

$$\mathbf{F}_m^0 = [\mathbf{F}_t^0; \mathbf{F}_v^n], \quad (5)$$

$$\mathbf{F}_m^{i+1} = L_i(\mathbf{F}_m^i), \quad (6)$$

$$M' = \mathcal{F}_d(\mathbf{F}_m^n, \mathbf{F}_t \mathbf{W}_o). \quad (7)$$

Here,  $L_i$  denotes the  $i$ -th Transformer layer of visual backbone, and  $\mathbf{W}_o \in \mathbb{R}^{d \times d}$  is the projection weight.  $[ \cdot ]$  denotes concatenation.  $M'$  is the predicted binary mask.

Considering the case of freezing SAM’s backbone, Eq.4 only adds a few parameters for semantic projection. Meanwhile, when the hidden Transformer layers are frozen, the inserted text tokens do not fit well into visual space. For the output of each layer, we also add a linear projection to facilitate text adaption, as shown in Fig. 3.

### 3.3. Layer-wise Instruction Tuning

According to Wu et al. (2023b), it is often difficult for additionally inserted tokens to fully interact with the existing sequences in the well learned semantic space, especially under the end-to-end transformations. We consider the layer-wise text instruction tuning for SAM, demoted as L-DIT.

Table 1: Comparison of different text-instructed schemes on RefCOCO. *Default* refers to the default lightweight fusion scheme of SAM. “*Add dec layers*” is to increasing the depth of the mask decoder. \* denotes that the image backbone is frozen, while the text and mask decoders are tuned. The best and second best performances are in **bold** and underlined.

Method	val						testA						testB					
	P@0.5	P@0.7	P@0.9	oIoU	mIoU	P@0.5	P@0.7	P@0.9	oIoU	mIoU	P@0.5	P@0.7	P@0.9	oIoU	mIoU	P@0.5	P@0.7	P@0.9
Default	72.20	59.56	18.78	60.74	63.41	75.28	63.76	18.76	62.95	65.65	66.95	52.63	19.82	56.69	59.95			
Default*	64.77	51.92	16.82	55.67	57.98	68.29	56.47	16.86	58.56	60.85	61.32	46.66	17.35	52.98	55.74			
Add 2 dec layers	80.80	71.65	27.03	67.17	70.51	83.52	75.27	25.48	69.63	72.48	76.57	65.19	29.24	64.04	67.61			
Add 2 dec layers*	71.44	59.03	18.61	59.88	62.88	75.34	63.06	18.29	62.77	65.55	66.48	52.41	19.78	56.79	59.80			
Add 4 dec layers	79.58	70.21	26.45	65.34	69.51	82.27	73.68	25.39	67.82	71.44	74.23	63.78	28.28	62.28	66.02			
Add 4 dec layers*	71.37	58.79	18.52	59.46	62.54	74.26	63.07	19.12	62.05	65.02	65.48	51.43	19.60	55.62	58.86			
End-to-end DIT	<b>81.78</b>	<u>73.07</u>	<b>28.27</b>	<u>68.07</u>	<b>71.46</b>	85.28	<u>77.17</u>	<b>27.56</b>	<u>70.81</u>	<b>73.90</b>	78.02	<u>67.60</u>	<b>30.20</b>	<u>65.58</u>	<b>69.36</b>			
End-to-end DIT*	76.51	66.00	23.19	62.96	66.87	78.89	68.41	21.31	63.74	67.83	72.90	60.01	25.39	60.43	64.63			
Layer-wise DIT	<b>85.68</b>	<b>76.61</b>	<b>29.89</b>	<b>71.98</b>	<b>74.73</b>	<b>88.06</b>	<b>79.17</b>	<u>25.94</u>	<b>74.51</b>	<b>75.62</b>	<b>81.28</b>	<b>69.11</b>	<b>30.95</b>	<b>68.77</b>	<b>71.21</b>			
Layer-wise DIT*	81.22	70.21	24.31	67.50	69.97	83.89	74.66	24.36	69.55	72.44	77.26	65.44	28.26	64.77	68.12			

Table 2: The combination with conventional prompt tuning. Here, *dynamic* refers to the projected text words changed according to different examples, *i.e.*, the setting of DITs, and *static* denotes the learnbale tokens.

Setting	Prompt	val				testA				testB						
		P@0.5	P@0.7	oIoU	mIoU	P@0.5	P@0.7	oIoU	mIoU	P@0.5	P@0.7	oIoU	mIoU			
End-to-end	dynamic	81.78	73.07	68.07	71.46	85.28	77.17	70.81	73.90	78.02	67.60	65.58	69.36			
End-to-end	dynamic+static	<u>82.60</u>	<u>73.89</u>	<u>68.53</u>	<u>72.11</u>	85.76	<u>77.76</u>	<u>71.21</u>	<u>74.12</u>	<u>78.41</u>	<u>67.39</u>	<u>65.64</u>	<u>69.38</u>			
Layer-wise	dynamic	<b>85.68</b>	<b>76.61</b>	<b>29.89</b>	<b>71.98</b>	<b>74.73</b>	<b>88.06</b>	<b>79.17</b>	<b>74.51</b>	<b>75.62</b>	<b>81.28</b>	<b>69.11</b>	<b>30.95</b>	<b>68.77</b>	<b>71.21</b>	
Layer-wise	dynamic+static	81.09	71.46	67.31	70.84	83.83	75.30	69.54	72.78	76.84	65.70	63.97	67.98			

Concretely, we insert the text prompts to the sub-semantic space of each Transformer layer of SAM’s encoder, thereby mitigating the modality gap for better tuning. Given the text features  $\mathbf{F}_t$ , we linearly project them to each layer of the image encoder, *i.e.*,  $\mathbf{F}_t^i$ , and the input sequence is defined by

$$\mathbf{F}_m^i = [\mathbf{F}_t^i; \mathbf{F}_v^i], \quad (8)$$

where  $i$  denotes the  $i$ -th layer.

Similar to Eq. 5-7, the final output visual tokens  $\mathbf{F}_v^k$  as well as the projected text features  $\mathbf{F}_t'$  are fed to the lightweight decoder for mask prediction. Compared with E-DIT, this layer-wise scheme can better adapt text prompts to the sub-spaces of SAM’s encoder, thereby improving the efficiency of text instruction tuning.

## 4. Experiments

To validate the proposed DITs, we conduct extensive experiments on three benchmark datasets of RIS, *i.e.*, RefCOCO (Yu et al., 2016), RefCOCO+ (Yu et al., 2016) and RefCOCOg (Mao et al., 2016), and also compare L-DIT with a bunch of state-of-the-art (SOTA) methods in RIS (Zhu et al., 2022; Yang et al., 2022; Liu et al., 2023b;d).

### 4.1. Datasets

**RefCOCO** (Yu et al., 2016) dataset is collected in an interactive two-player game (Kazemzadeh et al., 2014). There are 142,210 referring expressions and 50,000 segmentation masks in 19,994 images collected from COCO (Lin et al., 2014). It is divided into *train*, *val*, *testA*, and *testB* with 120,624, 10,834, 5,657, and 5,059 samples, respectively.

**RefCOCO+** (Yu et al., 2016) contains 141,564 natural language expressions and 49,856 masks in 19,992 images. Compared to RefCOCO, expressions in RefCOCO+ describe more about attributes of the referent, *e.g.*, color, shape, digits, and avoid using words of absolute spatial location such as *left* and *right*.

**RefCOCOg** (Mao et al., 2016; Nagaraja et al., 2016) has 104,560 expressions for 54,822 objects in 26,711 images. The expressions of RefCOCOg contain 8.4 words on average while that of RefCOCO and RefCOCO+ is only 3.6 and 3.5 words. It includes object appearance and location.

### 4.2. metrics

We use the *overall intersection-over-union* (oIoU), the *mean intersection-over-union* (mIoU), and *precision* at threshold of 0.5, 0.7, and 0.9 as evaluation metrics. The oIoU is mea-

Table 3: The impact of freezing the visual and text encoders. Here,  $\checkmark$  means that the encoder is frozen, while  $\times$  is updated.

Visual	Text	Method	val				testA				testB						
			P@0.5	P@0.7	P@0.9	oIoU	mIoU	P@0.5	P@0.7	P@0.9	oIoU	mIoU	P@0.5	P@0.7	P@0.9	oIoU	mIoU
$\checkmark$	$\checkmark$	End-to-end	71.83	57.95	18.83	60.76	62.87	75.41	62.49	19.05	63.61	65.67	68.15	52.43	19.54	57.97	60.23
$\checkmark$	$\checkmark$	Layer-wise	80.93	69.26	25.00	67.16	69.56	81.64	71.33	23.00	68.24	70.60	73.98	61.01	25.29	62.70	65.59
$\checkmark$	$\times$	End-to-end	76.51	66.00	23.19	62.96	66.87	78.89	68.41	21.31	63.74	67.83	72.90	60.01	25.39	60.43	64.63
$\checkmark$	$\times$	Layer-wise	81.22	70.21	24.31	67.50	69.97	83.89	74.66	24.36	69.55	72.44	77.26	65.44	28.26	64.77	68.12
$\times$	$\times$	End-to-end	81.78	73.07	28.27	68.07	71.46	85.28	77.17	27.56	70.81	73.90	78.02	67.60	30.20	65.58	69.36
$\times$	$\times$	Layer-wise	<b>85.68</b>	<b>76.61</b>	<b>29.89</b>	<b>71.98</b>	<b>74.73</b>	<b>88.06</b>	<b>79.17</b>	<b>25.94</b>	<b>74.51</b>	<b>75.62</b>	<b>81.28</b>	<b>69.11</b>	<b>30.95</b>	<b>68.77</b>	<b>71.21</b>

Table 4: The impact of different text words injections for L-DIT. *CrossAtt* and *FFN* refer to multi-head cross attention and feed-forward network (Vaswani et al., 2017), respectively. Linear projection is the setting of L-DIT.

Setting	val				testA				testB							
	P@0.5	P@0.7	P@0.9	oIoU	mIoU	P@0.5	P@0.7	P@0.9	oIoU	mIoU	P@0.5	P@0.7	P@0.9	oIoU	mIoU	
Linear project	<b>85.68</b>	<b>76.61</b>	<b>29.89</b>	<b>71.98</b>	<b>74.73</b>	<b>88.06</b>	<b>79.17</b>	<b>25.94</b>	<b>74.51</b>	<b>75.62</b>	<b>81.28</b>	<b>69.11</b>	<b>30.95</b>	<b>68.77</b>	<b>71.21</b>	
CrossAtt	80.49	70.70	25.63	67.06	70.33	83.30	73.45	24.43	69.67	72.01	76.98	65.33	28.08	64.85	68.13	
CrossAtt + FFN	82.07	72.22	27.09	68.26	71.42	84.96	76.29	<b>26.25</b>	71.03	73.52	78.34	66.29	29.43	65.68	69.00	

sured by the ratio of the total area of intersection to the total area of union across all test samples. The metric favors large objects over small ones. The mIoU is calculated as the average of the IoU values between predictions and the ground truth for all test samples. This measure is applied uniformly to both large and small objects.

#### 4.3. Implementation Details

For visual backbone, we use ViT-B/16, initialized from pre-trained weights of SAM. BERT with 12 layers and a hidden dimension of 768 is used as language encoder. We keep the aspect ratio and resize the image to 512 x 512. Following this, we apply color augmentation, Gaussian blur and random horizontal flipping to augment the data. To binarize the prediction of RIS, we set a threshold of 0.35. The optimizer is Adam with a learning rate of 1e-4, which is multiplied by a decay factor of 0.2 at the 30th and the 35th, and the batch size is set to 64. The warm-up epoch is configured to 3. The training process spans 40 epochs.

#### 4.4. Quantitative analysis

##### 4.4.1. COMPARISON WITH THE DEFAULT SCHEME

In Tab. 1, we first compare our *deep instruction tuning* (DIT) methods with the default fusion scheme of SAM and its alternatives, *i.e.*, adding more layers to the mask decoder. We can first see that the default fusion scheme performs much worse than DITs on RefCOCO under the setting of either fully tuning or freezing backbone, suggesting that the default lightweight decoder is insufficient in image-text

interactions. With more decoding layers, this issue can be alleviated to some extent, but the performance still lags behind DITs especially when the image encoder is frozen. To explain, the additional fusion layers can enhance the cross-modal interactions, but also undermines the powerful segmentation capability of SAM pre-trained on large amounts of data. In contrast, without modifying the main structure of SAM, our DIT methods can improve the performance greatly. Another interesting finding from Tab. 1 is that the advantage of layer-wise DIT is more obvious under the setting of freezing backbone. This result confirms our assumption that the layer-wise projection can better help to project text tokens onto the semantic space of SAM. Overall, Tab. 1 well validates the effectiveness of DITs for text-instructed SAM.

##### 4.4.2. ABLATION STUDY

**Combination with prompt tuning.** Tab. 2 present the results of combining DITs with conventional prompt tuning (Zhou et al., 2022a;b; Wu et al., 2023b), *i.e.*, adding learnable tokens to the text prompts. Under end-to-end tuning, the addition of learnable tokens can improve performance to a certain extent, mainly by increasing the parameter capacity of DIT for better text tuning. However, these prompt tokens are not helpful for layer-wise DIT, on the contrary, reducing performance greatly. This result may suggest that the text words are well projected onto each layer with independent projectors. The addition of parameterized tokens somewhat declines their semantics.

**The effect of freezing encoders.** In Tab. 3, we also ablate DITs under the parameter efficient setting (Zhou et al.,

Table 5: Comparison with the state-of-the-art methods on three RIS datasets. Here, *Scratch* refers to the models only tuned with RIS examples of these datasets, while *Pre-trained* denotes the use of a large number of visual grounding examples (Krishna et al., 2017) for pre-training. The metric used is oIoU.

Method	Visual Backbone	Textual Encoder	RefCOCO			RefCOCO+			RefCOCOg	
			val	testA	testB	val	testA	testB	val	test
<i>Trained from scratch:</i>										
MCN (Luo et al., 2020b)	Darknet53	bi-GRU	62.44	64.20	59.71	50.62	54.99	44.69	49.22	49.40
EFN (Feng et al., 2021)	ResNet101	bi-GRU	62.76	65.69	59.67	51.50	55.24	43.01	-	-
BUSNet (Yang et al., 2021)	DeepLab-R101	Self-Att	63.27	66.41	61.39	51.76	56.87	44.13	-	-
CGAN (Luo et al., 2020a)	DeepLab-R101	bi-GRU	64.86	68.04	62.07	51.03	55.51	44.06	51.01	51.69
ISFP (Liu et al., 2022)	Darknet53	bi-GRU	65.19	68.49	62.73	52.70	56.77	46.39	52.67	53.00
LST (Jing et al., 2021)	Darknet53	bi-GRU	65.43	67.76	63.08	54.21	58.32	48.02	54.40	54.25
ReSTR (Kim et al., 2022)	ViT-B	Transformer	67.22	69.30	64.45	55.78	60.44	48.27	-	-
LAVT (Yang et al., 2022)	Swin-B	BERT	72.73	75.82	68.79	62.14	68.38	55.10	61.24	62.09
VLT (Ding et al., 2022)	Swin-B	BERT	72.96	75.96	69.60	63.53	68.43	56.92	63.49	66.22
VDP (Zhao et al., 2023)	VQGAN	CLIP	73.25	-	-	62.69	-	-	61.96	-
ReLA (Liu et al., 2023b)	Swin-B	BERT	73.82	76.48	70.18	66.04	71.02	57.65	65.00	65.97
SADLR (Yang et al., 2023)	Swin-B	BERT	74.24	76.25	70.06	64.28	69.09	55.19	63.60	63.56
<i>Pre-trained:</i>										
MaLT (Li et al., 2021)	ViLT	BERT	70.13	71.71	66.92	62.23	65.92	56.06	62.45	62.87
CRIS (Wang et al., 2022)	CLIP-R101	CLIP	70.47	73.18	66.10	62.27	68.08	53.68	59.87	60.36
ETRIS (Xu et al., 2023b)	CLIP-R101	CLIP	71.06	74.11	66.66	62.23	68.51	52.79	60.28	60.42
SeqTR (Zhu et al., 2022)	Darknet53	bi-GRU	71.70	73.31	69.82	63.04	66.73	58.97	64.69	65.74
SEEM (Zou et al., 2024)	DaViT-d5	Florence	-	-	-	-	-	-	65.70	-
LISA-7B (Lai et al., 2023)	ViT-H	LLaVA-7B	74.90	<b>79.10</b>	72.30	65.10	70.80	58.10	<b>67.90</b>	<b>70.60</b>
PolyFormer (Liu et al., 2023d)	Swin-L	BERT	<b>75.96</b>	<b>78.29</b>	<b>73.25</b>	<b>69.33</b>	<b>74.56</b>	<b>61.87</b>	<b>69.20</b>	<b>70.19</b>
<i>Layer-wise DIT<sub>B</sub> (Ours)</i>	ViT-B	BERT	71.98	74.51	68.77	59.97	65.52	51.72	60.18	61.15
<i>Layer-wise DIT<sub>H</sub> (Ours)</i>	ViT-H	BERT	<b>76.18</b>	78.13	<b>73.27</b>	<b>68.00</b>	<b>71.77</b>	<b>60.04</b>	67.37	67.92

2022a;b; Luo et al., 2023). It can be seen that when freezing the SAM’s image backbone and the directly plugged-in BERT, L-DIT can still achieve an oIoU of 67.16 on RefCOCO *val*, which is even much better than fully tuning the default SAM, as shown in Tab. 1. Unfreezing both encoders can greatly improve performance. But compared with the pre-trained BERT, the significance of updating image encoder is much more obvious, *e.g.*, +4.88 oIoU on *val*. This result suggests that in DIT, the image encoder is capable of visual feature learning and cross-modal interactions, well confirming our intuition about DIT.

**Different text word injections.** In our layer-wise DIT, we project the text prompts directly onto the visual space of each SAM’s layer. Here, we also test DIT with alternative manners in Tab. 4, such as *cross-attention* and *cross-attention+FFN*. Interestingly, these complex methods do not further enhance SAM’s text-aware capability, but declining performance to some extent. This case suggests that with the strong dependency modeling of SAM’s ViT encoder, a direct semantic projection can well facilitate cross-modal alignment, well confirming the motivation of our DIT.

#### 4.5. Comparison with the State-of-the-art

In Tab. 5, we compare our L-DIT against the state-of-the-art (SOTA) methods of referring image segmentation on RefCOCO (Yu et al., 2016), RefCOCO+ (Yu et al., 2016), and RefCOCOg (Mao et al., 2016) datasets using the oIoU metric. Specially, on RefCOCO dataset, we outperforms existing trained from scratch SOTA methods with a absolute improvements of 1.94%, 1.56%, 2.91% in all three splits and performs on par with pretrained PolyFormer (Liu et al., 2023d). Furthermore, on RefCOCO+ and RefCOCOg datasets, the L-DIT<sub>H</sub> also exhibits exceptional performance, demonstrating comparable capabilities to SOTAs (Liu et al., 2023d; Yang et al., 2023). In addition, compared with SOTA RIS methods using a large number of visual grounding data for pre-training, Our L-DIT<sub>H</sub> is also very competitive and even achieves new SOTA performance on RefCOCO *val*.

#### 4.6. Qualitative Analysis

To gain deep insights into DIT, we visualize the predictions of our DIT tuning methods and SAM in Fig.4. In the first



Figure 4: Predictions of the default SAM and our end-to-end and layer-wise DITs, *i.e.*, E-DIT and L-DIT. Both methods can follow the text instruction better than the default SAM, while L-DIT can accurately segment the referent even with complex text content or image background. For better comparison, we use red boxes to ground the failed segmentations.

column, it becomes evident that the default SAM struggles with a nuanced understanding of text, often yielding predictions that inadequately encapsulate the referent or outright incorrect. In contrast, the simple E-DIT offers a notable improvement in SAM’s text comprehension capabilities. For instance, in the third example, SAM’s segmentation exhibit a pronounced bias towards the distracting elements on the left, while E-DIT rectifies this issue, resulting in more accurate prediction. Notably, through E-DIT enhances the performance in some cases, it can lead to the loss of certain semantic information embedded within the textual features. As a consequence, E-DIT can occasionally misinterpret the segmentation target, as illustrated in the last example. The last column reveals that L-DIT effectively mitigates these issues without necessitating specific designs for cross-modal features. Remarkably, even without providing explicit image positions, akin to the original SAM, L-DIT consistently delivers superior segmentation results. This demonstrates that L-DIT processing can effectively harness positional information from both modalities and maintain a strong degree of context-awareness, improving accuracy and robustness.

## 5. Conclusion

In this paper, we propose two deep instruction tuning (DIT) methods to address the weakness of SAM on following text instructions. One is end-to-end and the other is layer-wise. DITs regard SAM’s default visual encoder as a stand-alone multi-modal learner instead of adding additional fusion branches. Both approaches contribute to enhancing SAM’s ability to position segmented objects based on textual guidance. To validate DITs, we conduct extensive experiments on three RIS benchmark datasets. Experimental results show that our simple DIT methods can greatly improve the capabilities of SAM. Meanwhile, the proposed layer-wise DIT can even help SAM compete with a set of SOTA methods on RIS on all three datasets.

## 6. Broader Impact

This paper reveals the key drawbacks of SAM in text-guided segmentation, and propose two simple yet effective deep instruction tuning methods for SAM. The findings and methods of this paper can further advance the development of SAM in the machine learning community. There are many potential societal consequences of our work, none of which we

feel must be specifically highlighted here.

**Acknowledgements.** This work was supported by National Science and Technology Major Project (No. 2022ZD0118201), the National Science Fund for Distinguished Young Scholars (No.62025603), the National Natural Science Foundation of China (No. U21B2037, No. U22B2051, No. 62176222, No. 62176223, No. 62176226, No. 62072386, No. 62072387, No. 62072389, No. 62002305 and No. 62272401), and the Natural Science Foundation of Fujian Province of China (No.2021J01002, No.2022J06001).

## References

Badrinarayanan, V., Kendall, A., and Cipolla, R. Segnet: A deep convolutional encoder-decoder architecture for image segmentation. *TPAMI*, 2017.

Chen, L.-C., Papandreou, G., Kokkinos, I., Murphy, K., and Yuille, A. L. Deeplab: Semantic image segmentation with deep convolutional nets, atrous convolution, and fully connected crfs. *TPAMI*, 2017.

Deng, J., Yang, Z., Chen, T., Zhou, W., and Li, H. Transvg: End-to-end visual grounding with transformers. In *ICCV*, 2021.

Devlin, J., Chang, M.-W., Lee, K., and Toutanova, K. Bert: Pre-training of deep bidirectional transformers for language understanding. *arXiv*, 2018.

Ding, H., Liu, C., Wang, S., and Jiang, X. Vlt: Vision-language transformer and query generation for referring segmentation. *TPAMI*, 2022.

Dosovitskiy, A., Beyer, L., Kolesnikov, A., Weissenborn, D., Zhai, X., Unterthiner, T., Dehghani, M., Minderer, M., Heigold, G., Gelly, S., et al. An image is worth 16x16 words: Transformers for image recognition at scale. *arXiv*, 2020.

Feng, G., Hu, Z., Zhang, L., and Lu, H. Encoder fusion network with co-attention embedding for referring image segmentation. In *CVPR*, 2021.

Gu, Y., Han, X., Liu, Z., and Huang, M. Ppt: Pre-trained prompt tuning for few-shot learning. *arXiv*, 2021.

Han, X., Zhao, W., Ding, N., Liu, Z., and Sun, M. Ptr: Prompt tuning with rules for text classification. *AI Open*, 2022.

He, K., Gkioxari, G., Dollár, P., and Girshick, R. Mask r-cnn. In *ICCV*, 2017.

Hu, R., Rohrbach, M., and Darrell, T. Segmentation from natural language expressions. In *ECCV*, 2016.

Hu, Y., Wang, Q., Shao, W., Xie, E., Li, Z., Han, J., and Luo, P. Beyond one-to-one: Rethinking the referring image segmentation. In *ICCV*, 2023.

Huang, S., Hui, T., Liu, S., Li, G., Wei, Y., Han, J., Liu, L., and Li, B. Referring image segmentation via cross-modal progressive comprehension. In *CVPR*, 2020.

Jia, M., Tang, L., Chen, B.-C., Cardie, C., Belongie, S., Hariharan, B., and Lim, S.-N. Visual prompt tuning. In *ECCV*, 2022.

Jing, Y., Kong, T., Wang, W., Wang, L., Li, L., and Tan, T. Locate then segment: A strong pipeline for referring image segmentation. In *CVPR*, 2021.

Kazemzadeh, S., Ordonez, V., Matten, M., and Berg, T. Referitgame: Referring to objects in photographs of natural scenes. In *EMNLP*, 2014.

Kim, N., Kim, D., Lan, C., Zeng, W., and Kwak, S. Restr: Convolution-free referring image segmentation using transformers. In *CVPR*, 2022.

Kim, W., Son, B., and Kim, I. Vilt: Vision-and-language transformer without convolution or region supervision. In *ICML*, 2021.

Kirillov, A., He, K., Girshick, R., Rother, C., and Dollár, P. Panoptic segmentation. In *CVPR*, 2019.

Kirillov, A., Mintun, E., Ravi, N., Mao, H., Rolland, C., Gustafson, L., Xiao, T., Whitehead, S., Berg, A. C., Lo, W.-Y., et al. Segment anything. *arXiv*, 2023.

Krishna, R., Zhu, Y., Groth, O., Johnson, J., Hata, K., Kravitz, J., Chen, S., Kalantidis, Y., Li, L.-J., Shamma, D. A., et al. Visual genome: Connecting language and vision using crowdsourced dense image annotations. *IJCV*, 2017.

Lai, X., Tian, Z., Chen, Y., Li, Y., Yuan, Y., Liu, S., and Jia, J. Lisa: Reasoning segmentation via large language model. *arXiv*, 2023.

Lee, D., Song, S., Suh, J., Choi, J., Lee, S., and Kim, H. J. Read-only prompt optimization for vision-language few-shot learning. In *ICCV*, 2023.

Li, L. H., Zhang, P., Zhang, H., Yang, J., Li, C., Zhong, Y., Wang, L., Yuan, L., Zhang, L., Hwang, J.-N., et al. Grounded language-image pre-training. In *CVPR*, 2022.

Li, M. and Sigal, L. Referring transformer: A one-step approach to multi-task visual grounding. *NeurIPS*, 2021.

Li, R., Li, K., Kuo, Y.-C., Shu, M., Qi, X., Shen, X., and Jia, J. Referring image segmentation via recurrent refinement networks. In *CVPR*, 2018.

Li, Y., Chen, X., Zhu, Z., Xie, L., Huang, G., Du, D., and Wang, X. Attention-guided unified network for panoptic segmentation. In *CVPR*, 2019.

Li, Z., Wang, M., Mei, J., and Liu, Y. Mail: A unified mask-image-language trimodal network for referring image segmentation. *arXiv*, 2021.

Lin, T.-Y., Maire, M., Belongie, S., Hays, J., Perona, P., Ramanan, D., Dollár, P., and Zitnick, C. L. Microsoft coco: Common objects in context. In *ECCV*, 2014.

Liu, C., Lin, Z., Shen, X., Yang, J., Lu, X., and Yuille, A. Recurrent multimodal interaction for referring image segmentation. In *ICCV*, 2017.

Liu, C., Jiang, X., and Ding, H. Instance-specific feature propagation for referring segmentation. *ACM MM*, 2022.

Liu, C., Ding, H., and Jiang, X. Gres: Generalized referring expression segmentation. In *CVPR*, 2023a.

Liu, C., Ding, H., and Jiang, X. Gres: Generalized referring expression segmentation. In *CVPR*, 2023b.

Liu, D., Zhang, H., Wu, F., and Zha, Z.-J. Learning to assemble neural module tree networks for visual grounding. In *ICCV*, 2019.

Liu, J., Ding, H., Cai, Z., Zhang, Y., Satzoda, R. K., Mahadevan, V., and Manmatha, R. Polyformer: Referring image segmentation as sequential polygon generation. In *CVPR*, 2023c.

Liu, J., Ding, H., Cai, Z., Zhang, Y., Satzoda, R. K., Mahadevan, V., and Manmatha, R. Polyformer: Referring image segmentation as sequential polygon generation. In *CVPR*, 2023d.

Liu, P., Yuan, W., Fu, J., Jiang, Z., Hayashi, H., and Neubig, G. Pre-train, prompt, and predict: A systematic survey of prompting methods in natural language processing. *ACM CSUR*, 2023e.

Liu, X., Ji, K., Fu, Y., Tam, W. L., Du, Z., Yang, Z., and Tang, J. P-tuning v2: Prompt tuning can be comparable to fine-tuning universally across scales and tasks. *arXiv*, 2021.

Liu, Y., Zhang, C., Wang, Y., Wang, J., Yang, Y., and Tang, Y. Universal segmentation at arbitrary granularity with language instruction. *arXiv*, 2023f.

Long, J., Shelhamer, E., and Darrell, T. Fully convolutional networks for semantic segmentation. In *CVPR*, 2015.

Luo, G., Zhou, Y., Ji, R., Sun, X., Su, J., Lin, C.-W., and Tian, Q. Cascade grouped attention network for referring expression segmentation. In *ACM MM*, 2020a.

Luo, G., Zhou, Y., Sun, X., Cao, L., Wu, C., Deng, C., and Ji, R. Multi-task collaborative network for joint referring expression comprehension and segmentation. In *CVPR*, 2020b.

Luo, G., Huang, M., Zhou, Y., Sun, X., Jiang, G., Wang, Z., and Ji, R. Towards efficient visual adaption via structural re-parameterization. *arXiv*, 2023.

Mao, J., Huang, J., Toshev, A., Camburu, O., Yuille, A. L., and Murphy, K. Generation and comprehension of unambiguous object descriptions. In *CVPR*, 2016.

Margffoy-Tuay, E., Pérez, J. C., Botero, E., and Arbeláez, P. Dynamic multimodal instance segmentation guided by natural language queries. In *ECCV*, 2018.

Nagaraja, V. K., Morariu, V. I., and Davis, L. S. Modeling context between objects for referring expression understanding. In *ECCV*, 2016.

Ouyang, L., Wu, J., Jiang, X., Almeida, D., Wainwright, C., Mishkin, P., Zhang, C., Agarwal, S., Slama, K., Ray, A., et al. Training language models to follow instructions with human feedback. *NeurIPS*, 2022.

Ronneberger, O., Fischer, P., and Brox, T. U-net: Convolutional networks for biomedical image segmentation. In *MICCAI*, 2015.

Tian, Z., Shen, C., and Chen, H. Conditional convolutions for instance segmentation. In *ECCV*, 2020.

Touvron, H., Lavril, T., Izacard, G., Martinet, X., Lachaux, M.-A., Lacroix, T., Rozière, B., Goyal, N., Hambro, E., Azhar, F., et al. Llama: Open and efficient foundation language models. *arXiv*, 2023.

Vaswani, A., Shazeer, N., Parmar, N., Uszkoreit, J., Jones, L., Gomez, A. N., Kaiser, Ł., and Polosukhin, I. Attention is all you need. *NeurIPS*, 2017.

Wang, X., Zhang, R., Kong, T., Li, L., and Shen, C. Solov2: Dynamic and fast instance segmentation. *NeurIPS*, 2020.

Wang, Z., Lu, Y., Li, Q., Tao, X., Guo, Y., Gong, M., and Liu, T. Cris: Clip-driven referring image segmentation. In *CVPR*, 2022.

Wei, J., Bosma, M., Zhao, V. Y., Guu, K., Yu, A. W., Lester, B., Du, N., Dai, A. M., and Le, Q. V. Finetuned language models are zero-shot learners. *arXiv*, 2021.

Wu, J., Jiang, Y., Yan, B., Lu, H., Yuan, Z., and Luo, P. Segment every reference object in spatial and temporal spaces. In *ICCV*, 2023a.

Wu, Q., Huang, S., Zhou, Y., Dai, P., Shu, A., Jiang, G., and Ji, R. Approximated prompt tuning for vision-language pre-trained models. *arXiv*, 2023b.

Xie, E., Wang, W., Yu, Z., Anandkumar, A., Alvarez, J. M., and Luo, P. Segformer: Simple and efficient design for semantic segmentation with transformers. *NeurIPS*, 2021.

Xu, L., Huang, M. H., Shang, X., Yuan, Z., Sun, Y., and Liu, J. Meta compositional referring expression segmentation. In *CVPR*, 2023a.

Xu, Z., Chen, Z., Zhang, Y., Song, Y., Wan, X., and Li, G. Bridging vision and language encoders: Parameter-efficient tuning for referring image segmentation. In *ICCV*, 2023b.

Yan, B., Jiang, Y., Wu, J., Wang, D., Luo, P., Yuan, Z., and Lu, H. Universal instance perception as object discovery and retrieval. In *CVPR*, 2023.

Yang, S., Xia, M., Li, G., Zhou, H.-Y., and Yu, Y. Bottom-up shift and reasoning for referring image segmentation. In *CVPR*, 2021.

Yang, Z., Wang, J., Tang, Y., Chen, K., Zhao, H., and Torr, P. H. Lavt: Language-aware vision transformer for referring image segmentation. In *CVPR*, 2022.

Yang, Z., Wang, J., Tang, Y., Chen, K., Zhao, H., and Torr, P. H. Semantics-aware dynamic localization and refinement for referring image segmentation. *arXiv*, 2023.

Yu, L., Poirson, P., Yang, S., Berg, A. C., and Berg, T. L. Modeling context in referring expressions. In *ECCV*, 2016.

Zhao, W., Rao, Y., Liu, Z., Liu, B., Zhou, J., and Lu, J. Unleashing text-to-image diffusion models for visual perception. *arXiv*, 2023.

Zhou, K., Yang, J., Loy, C. C., and Liu, Z. Conditional prompt learning for vision-language models. In *CVPR*, 2022a.

Zhou, K., Yang, J., Loy, C. C., and Liu, Z. Learning to prompt for vision-language models. *IJCV*, 2022b.

Zhu, C., Zhou, Y., Shen, Y., Luo, G., Pan, X., Lin, M., Chen, C., Cao, L., Sun, X., and Ji, R. Seqtr: A simple yet universal network for visual grounding. In *ECCV*, 2022.

Zou, X., Yang, J., Zhang, H., Li, F., Li, L., Wang, J., Wang, L., Gao, J., and Lee, Y. J. Segment everything everywhere all at once. *NeurIPS*, 2024.